Winter methane fluxes over boreal and Arctic environments

Alex Mavrovic[1–2–3–4], Oliver Sonnentag[2–4], Juha Lemmetyinen[5], Carolina Voigt[4–6], Mika Aurela[5], Alexandre Roy[1–2]

[1]Université du Québec à Trois–Rivières, Département des sciences de l'environnement, Trois–Rivières, Québec, G9A 5H7, Canada

[2]Centre d'Études Nordiques, Québec, Québec, G1V 0A6, Canada

[3]Polar Knowledge Canada, Canadian High Arctic Research Station campus, Cambridge Bay, Nunavut, X0B 0C0, Canada

[4]Université de Montréal, Département de géographie, Montréal, Québec, H3T 1J4, Canada

[5]Finnish Meteorological Institute, Helsinki, FI–00560, Finland

[6]Universität Hamburg, 20146 Hamburg, Germany

Corresponding author: Alex Mavrovic (alex.mavrovic@uqtr.ca)

Key Points:

- Boreal forest upland soils acted as net methane sink during winter.
- Boreal wetland soils acted as net winter methane source, while tundra wetlands emissions were generally low except for a few hotspots.
- In boreal forests, the soil liquid water content was one of the main environmental controls on winter methane fluxes.

Keywords:

Methane flux, Methane exchange, Arctic–boreal regions, Carbon cycle, Winter, Non–growing season.

Abstract

Unprecedented warming of Arctic–boreal regions (ABR) has poorly understood consequences on carbon cycle processes. Uncertainties in annual methane (CH_4) budgets partly arise because of limited data availability during winter. In this study, winter CH_4 flux measurements were conducted using the snowpack diffusion gradient method over five ABR ecosystem types in Canada and Finland: closed–crown and open–crown coniferous boreal forest, boreal wetland and erect–shrub and prostrate–shrub tundra. Boreal forest uplands acted as net CH_4 sinks, while the boreal wetland acted as net CH_4 source during winter. We identified several wetland tundra CH_4 emission hotspots and large spatial variability in boreal wetland CH_4 emissions. In the boreal forest uplands, soil liquid water content was identified as an important environmental control of winter CH_4 fluxes. Our results indicate non–negligible winter CH_4 flux, which must be accounted for in annual carbon balance and terrestrial biosphere models over ABR.

Plain Language Summary

The climate of our planet is closely linked to the atmospheric concentrations of greenhouse gases such as carbon dioxide and methane that partially retain the energy coming from the Sun. The Arctic and boreal regions are some of the environments that have been the least studied, mostly because of their remoteness. In those environments, winter is the least studied period of the year because of technical challenges posed by harsh winter conditions. Our study focused on winter methane exchange between the snow–covered ground surface and the atmosphere in Arctic–boreal regions. Methane is found in smaller quantities in the atmosphere compared to carbon dioxide but with a much stronger warming potential. We observed that the boreal forests acted as a sink of methane, removing methane from the atmosphere during winter. In contrast, boreal wetlands emitted important amounts of methane into the atmosphere. We observed low methane emissions in the Arctic tundra except for a few hotspots with high methane emissions. All those observations show the variability of methane exchanges in different environments and highlight the importance of understanding those exchanges to improve our ability to predict the role of Arctic–boreal regions on the climate system.

1 Introduction

Methane (CH_4) exchange between the ground surface and the atmosphere in Arctic and boreal biomes (hereafter called Arctic–boreal regions; ABR) play an important role in the global climate with potentially important responses to a warming climate (Bekryaev et al., 2010; Kirschke et al., 2013; Yvon–Durocher et al., 2014; Schuur et al., 2015; Dean et al., 2018; Rößger et al., 2022). The response of ABR CH_4 fluxes to temperature is especially relevant since the ABR are warming up to four times faster than the rest of the planet (Derksen et al., 2019; Rantanen et al., 2022). The soils of ABR store a vast amount of labile organic matter due to inherently slow decomposition rates, largely attributable to cold temperatures (Tarnocai et al., 2009; Deluca and Boisvenue, 2012; Ravn et al., 2020). Therefore, altered CH_4 exchange rates due to ABR warming up could generate potentially non–negligible, positive feedback to the global climate system (Natali et al., 2021; Rößger et al., 2022; Schuur et al., 2022). Poor understanding of environmental controls on CH_4 exchange during winter constitutes a large source of uncertainty in the ABR CH_4 budget (McGuire et al., 2012; Mastepanov et al., 2013; Treat et al., 2018).

The net soil CH_4 flux is a result of three groups of processes: production, oxidation, and transport of CH_4. CH_4 in soils is produced by methanogens during organic matter decomposition under mostly anoxic conditions, which typically occur in deeper soil layers or in water–saturated environments (Zhang et al., 2017; Feng et al., 2020; Bastviken et al., 2023). In contrast, under predominantly aerobic conditions, CH_4 is oxidized by methanotrophs as a source of energy and carbon (Lai, 2009; Bastviken et al., 2023). Such aerobic conditions are often found in drier upper soil layers in mineral upland soils. In well–drained soils, CH_4 oxidation typically exceeds production resulting in a net soil CH_4 sink that removes CH_4 from the atmosphere (Lai, 2009; Lee et al., 2023). In contrast, CH_4 oxidation in wetlands is lower than production resulting in net CH_4 emissions (Topp and Pattey, 1997; Roslev et al., 1997). Still, CH_4 oxidation in wetlands is an important process that removes a large percentage of CH4 produced in saturated soil layers before it can reach the atmosphere (Oertel et al., 2016). During the oxidation process, CH_4 is oxidized to carbon dioxide (CO_2) and water (H_2O). Methane transport, i.e., the movement of CH_4 from its zone of production to the atmosphere by diffusion, ebullition, and plant–mediated transport also plays an important role in mitigating CH_4 oxidation by limiting the time during which methanotrophs can consume CH_4 (Bastviken et al., 2023). The vegetation composition of the ecosystem has been shown to impact CH_4 fluxes by providing the organic matter substrate for CH_4 production, bypassing zones of CH_4 oxidation by plant–mediated transport, and by its indirect impact on water table and thaw depth (King et al., 1998; Andresen et al., 2017; Bastviken et al., 2023).

The majority of prior CH_4 studies in the ABR has focused on snow–free growing season fluxes (e.g., Ullah et al., 2009; Zona et al., 2009; Helbig et al., 2016; Kuhn et al., 2021). The largest CH_4 flux measurement network, FLUXNET–CH4, provides limited winter data from ABR due to the failure of equipment in cold harsh conditions (Knox et al., 2019; Delwiche et al., 2021). The few studies on winter CH_4 fluxes in the Arctic biome that exist showed that winter can contribute up to 40 to 50% of the annual net CH_4 emissions (Zona et al., 2016; Treat et al., 2018; Rößger et al., 2022; Ito et al., 2023). The length of winter typically increases with latitude and can span the period from September to June. Most of the winter ABR CH_4 studies focus on wetlands and peatlands where higher emissions are expected, with little attention to CH_4 sinks (Treat et al., 2018). More studies of winter CH_4 fluxes have been carried out in the boreal biome than in the Arctic biome, but even in the boreal biome, winter CH4 flux measurements remain scarce compared to growing season studies (Viru et al., 2020; Hiyama et al., 2021; Lee et al., 2023). Overall, the limited data available on ABR CH_4 fluxes translates into limited knowledge of environmental controls of winter CH_4 fluxes. This lack of knowledge is challenging terrestrial biosphere models, often using CH_4 emission schemes developed for the growing season or lower latitudes and more temperate environments which can be inaccurate when extrapolated to the ABR carbon cycle (Fisher et al., 2014; Ito et al., 2023).

The goal of this study is to quantify winter CH_4 fluxes in different ABR ecosystems and identify environmental controls on fluxes. Our study is based on 660 snowpack diffusion gradient and supporting measurements (snowpack properties, soil temperature and liquid water content) at five different ecosystems in Arctic and boreal biomes in Finland and Canada: a boreal wetland, a closed–crown coniferous boreal forest stand, two open–crown coniferous boreal forest stands, an erect–shrub tundra, and a prostrate–shrub tundra site. Spatially distributed measurements of

snowpack CH_4 diffusion gradients were performed during the 2020–2021, 2021–2022 and 2022–2023 winters (December to May).

2 Materials and Methods

2.1 Measurements sites

Five study sites characteristic of five ABR ecosystems were selected (Fig. S1; Table S1 and S2). Cambridge Bay (CB; Nunavut, Canada) was the northernmost site located in the Arctic biome dominated by lichen and prostrate shrub tundra. The CB site is constituted of mesic areas (CB–mes) and wetland areas (CB–wet) (Ponomarenko et al., 2019), Trail Valley Creek (TVC; Northwest Territories, Canada) is situated in the forest–tundra ecotone, the transitional zone between the boreal and Arctic biomes. TVC is dominated by erect shrub tundra with remaining tree patches (Martin et al., 2022; Voigt et al., 2023). Havikpak Creek (HPC; Northwest Territories, Canada) is located about 50 km south of TVC in an open–crown black spruce dominated forest stand, just south of the treeline (Krogh et al., 2017). Sodankylä (SOD, Lapland, Finland) is in the northern boreal biome. The SOD study site comprises two study zones: a closed–crown Scots pine–dominated forest stand (SOD–for) and adjacent open wetlands (*aapa mire*; SOD–wet) (Ikonen et al., 2016). Montmorency Forest (MM; Québec, Canada) is the southernmost site located in a closed–crown balsam fir dominated boreal forest (Barry et al., 1988). The CB, TVC and HPC sites are underlain by continuous permafrost, while the MM and SOD sites are permafrost–free.

2.2 CH_4 flux calculation

In snow–covered regions, a vertical CH_4 diffusion gradient ($d[CH_4]/dz$; gC m^{-4}) is maintained through the snowpack as a result of CH_4 production, oxidation and transport in soils. Fick's first law for gas diffusion in porous media can be used to estimate CH_4 fluxes (F_{CH4}; mg C m^{-2} day^{-1}) from $d[CH_4]/dz$ (Sommerfeld et al., 1993; Zhu et al., 2014):

$$F_{CH4} = -\varphi \cdot \tau \cdot D \cdot \frac{d[CH_4]}{dz} \quad (1)$$

where φ represents the snow porosity (unitless), τ the snow tortuosity (unitless) and D the diffusion coefficient of CH_4 through the air in m^2 day^{-1}. φ and τ can be estimated from snow density (ρ_{snow}) and snow liquid water content (Θ) (Du Plessis and Masliyah 1991; Kinar and Pomeroy, 2015; Madore et al., 2022):

$$\varphi = 1 - \frac{\rho_{snow}}{\rho_{ice}} + \theta \cdot \left(\frac{\rho_{water}}{\rho_{ice}} - 1\right) \quad (2)$$

$$\tau = \frac{1-(1-\varphi)^{2/3}}{\varphi} \approx \varphi^{1/3} \quad (3)$$

where ρ represents the density of snow, pure ice and water in g cm^{-3} (ρ_{water} = 0.99984 g cm^{-3} at T = 0 °C; Harvey et al., 2017). Ice density (ρ_{ice}) must be adjusted for ice temperature (T_{ice}) (Harvey et al., 2017):

$$\rho_{ice} = -0.0001 \cdot T_{ice} + 0.9168 \quad (4)$$

Standard diffusion coefficients of CH_4 are available in literature but must be corrected for temperature and pressure (Marrero and Mason, 1972; Massman, 1988):

$$D = 0.1859 \cdot \left(\frac{T}{T_o}\right)^{1.747} \quad (5)$$

where T is the air temperature and T_o is the freezing point (273.15 K). The diffusion gradient method assumes that gas fluxes are the result of simple, linear, gradient–induced diffusion through snowpack porosities (McDowell et al., 2000). If the gas flow is altered by ice crusts or dense snow layers, it could lead to a positive bias (i.e., F_{CH4} overestimation; Seok et al., 2009). Such layers were rarely found in our study sites and did not cause the $d[CH_4]/dz$ to diverge from its linear relationship. In contrast, the diffusion gradient assumption also does not hold when strong wind events occur, decreasing snowpack CH_4 concentration through wind pumping and inducing a negative bias on CH_4 fluxes (Seok et al., 2009). Consequently, $d[CH_4]/dz$ was not measured in days following a strong wind event. Monitoring of F_{CH4} at a few sampling locations did not show any relationship between F_{CH4} and wind speed or atmospheric pressure (Mavrovic et al., 2023).

2.3 Data collection

The $d[CH_4]/dz$ was estimated by collecting gas samples along a vertical profile in the snowpack. Five gas samples were collected for each vertical profile: I) at 5 cm above the snowpack (ambient air), II) at 5 cm depth from the snowpack surface, III) at 1/3 of total snow depth, IV) at 2/3 of total snow depth and V) at the soil–snow interface. Snow pore gas was collected with a thin hollow stainless–steel rod (50–120 cm long, 4 mm outer diameter and 2 mm inner diameter). Gas was collected in a 60 mL syringe (Air–Tite Luer Lock, Virginia Beach, Virginia) connected to the rod via a three–way valve before being transferred into 12 mL hermetic glass vials (Labco Exetainer®, Labco Ltd., Lampeter, UK). CH_4 concentration was measured with a Licor LI–7810 $CH_4/CO_2/H_2O$ Trace Gas Analyzer ($\sigma < 0.03\%$ at 2 ppm; LI–COR Biosciences, Lincoln, Nebraska, US) using an open–loop method with a continuous flow of a 1.1 ppm CH_4 calibration gas (Linde Canada, Ottawa, Ontario). The CH_4 concentration of gas samples was calculated based on a calibration curve of gas standards ranging from 0 to 10 ppm of CH_4. At each site, several sampling locations were selected to cover the full range of vegetation types and snowpack characteristics, covering defined areas of 0.25–4 km^2. At each sampling location, 2 to 4 replicate profiles were measured within 2–3 m to ensure sampling repeatability.

After gas sampling, a vertical profile of snow and soil properties was measured to calculate snow porosity, tortuosity and the CH_4 diffusion coefficient. Snow properties were measured at every 5 cm including snow temperature (Snowmetrics digital thermometer; a tenth of a degree resolution), snow density (Snowmetrics digital scale, 100 and 250 cm^3 snow cutters; $\sigma(\rho_{snow}) \approx$ 9%; Proksch et al., 2016), snow liquid water content (hand test from Fierz et al., 2009) and snow stratigraphy. Near–surface soil temperature (T_{soil}) was measured at 1 cm depth below the soil–snow interface, and three measurements within 1 m of T_{soil} were averaged. An uncertainty assessment was conducted to evaluate CH_4 flux precision based on the snowpack diffusion gradient method; the detailed method can be found in the supporting information (Table S3 and Fig. S2). An empirical soil liquid water and ice mixing model following Zhang et al. (2010) was used to calculate soil volumetric liquid water content (LWC); the detailed calculation can be found in the supporting information.

3 Results

3.1 Winter methane fluxes across ABR sites

Our results showed mostly low to negligible CH_4 emissions in tundra sites (CB and TVC) and open–crown boreal forest (HCP). At those sites, fluxes ranged from –0.21 mg C m^{-2} day^{-1} (CH_4 uptake) to 0.33 mg C m^{-2} day^{-1} (CH_4 emissions) with a mean rate of 0.03 ± 0.08 mg C m^{-2} day^{-1} (mean ± standard deviation), except for a few hotspots at CB that emitted CH_4 up to 1.46 mg C m^{-2} day^{-1} with a mean rate of 0.78 ± 0.31 mg C m^{-2} day^{-1} (Fig. 1). The winter CH_4 hotspots were revisited 10 times over a period of 8 weeks and consistently displayed high CH_4 emissions.

Several vegetation types were found in the Arctic tundra sites of CB and TVC. The main differences between CH_4 fluxes among vegetation types at CB followed soil water regimes as divided into mesic and wetland areas (Fig. 1). We observed some differences in the ranges and means of CH_4 fluxes among TVC vegetation types, although those differences were small compared to the variability between study sites (Fig. S3). The TVC vegetation types surveyed by ascending mean CH_4 fluxes are as follows: dwarf shrub, black spruce patch, riparian shrub, lichen, tussock, polygon, and tall shrub. The closed–crown coniferous boreal forest sites showed mean CH_4 uptake rates throughout winter of –0.43 ± 0.34 mg C m^{-2} day^{-1} (MM) and –0.47 ± 0.26 mg C m^{-2} day^{-1} (SOF–for). The SOD–wet boreal wetland displayed high CH_4 emissions throughout winter, with rates up to 48.51 mg C m^{-2} day^{-1} and an average of 4.57 ± 7.34 mg C m^{-2} day^{-1}. The boreal wetland F_{CH4} at SOD–for were at least one order of magnitude higher than any other site in this study. The boreal wetland sampling locations displayed an important spatial variability of F_{CH4} with some sampling locations emitting CH_4 at average rates up to 50 times higher than the lowest ones (Fig. S4).

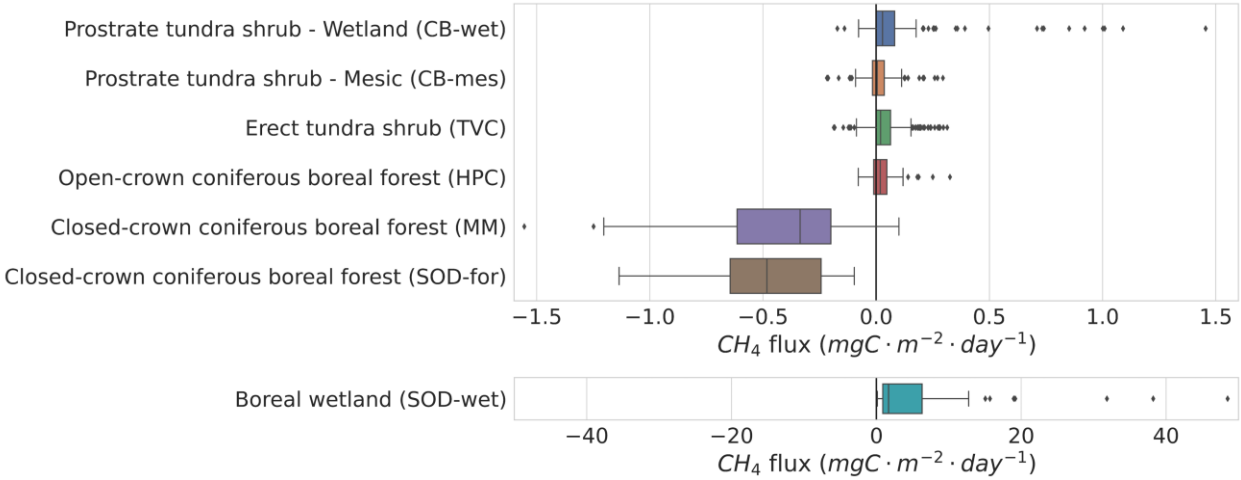

Figure 1. CH_4 flux across the study sites. Outliers were defined as F_{CH4} > Q3 + 1.5 IQR where Q3 is the third quartile and IQR the interquartile range. The F_{CH4} from the boreal wetland is shown on a separate axis since the range of F_{CH4} is of a different order of magnitude.

3.2 Environmental controls of winter methane fluxes

Statistical analyses were performed to identify the environmental variables (i.e., T_{soil}, soil LWC, vegetation type and snow variables) controlling CH_4 fluxes at both the site–level and over the entire dataset in the different northern ecosystems. The statistical analysis approach included correlation, regression and machine learning (i.e., Random Forest). For tundra sites (i.e., CB and TVC), as the CH_4 fluxes were relatively small, none of these variables proved statistically significant (e.g., Fig. 3 for T_{soil}). The correlation between F_{CH4} and snow variables was low at all study sites ($R^2 < 0.13$ for total snow height, SWE and mean snow density). However, at the closed–crown coniferous boreal forest sites of MM and SOD–for, our results show a site–specific linear relationship between winter F_{CH4} and soil LWC (Fig. 2). The correlation between F_{CH4} and T_{soil} at 1 cm depth was low since T_{soil} had a narrow range during the measurement campaigns at MM and SOD–for, being around freezing point for all measurements ($R^2 = 0.035$; Fig. 3). MM and SOD–for boreal forest uplands were the only two sites with near–surface T_{soil} close enough to 0°C to allow the coexistence of ice and liquid water in the soil. Water–saturated organic layers also occurred at the boreal wetland of SOD–wet, but the liquid water was trapped under a top–layer made mostly of solid ice with a thickness of several centimeters.

One sampling location at MM displayed different soil properties than the other sampling locations because of its thick organic soil layer and high soil moisture regime due to its location near the bottom of a microtopographic depression (Fig. 2). Other MM sampling locations with a thin organic layer shared a similar soil composition dominated by sandy loam mineral soils. The MM thick organic layer sampling location alternates between a CH_4 source or sink throughout the snow–covered season.

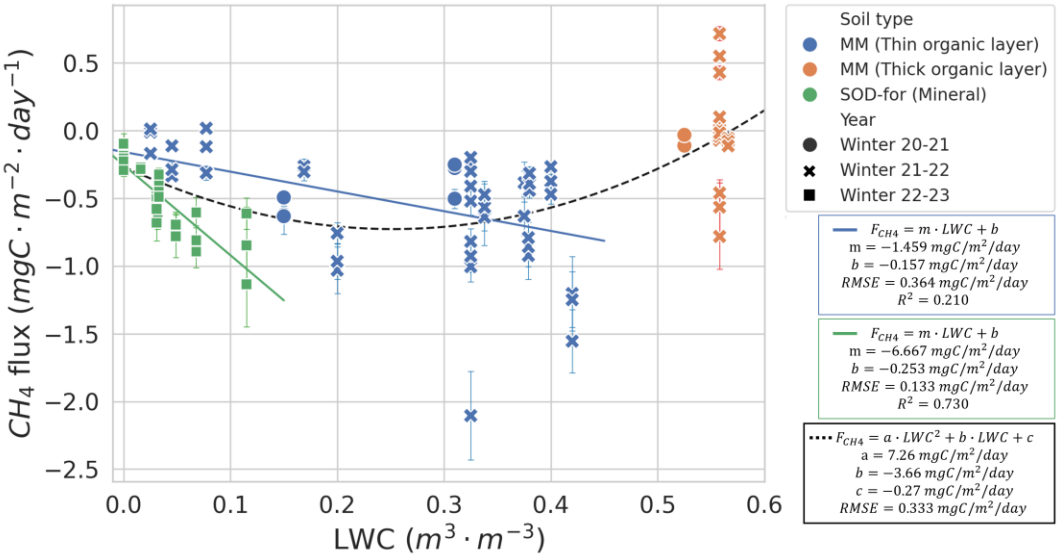

Figure 2. CH_4 flux as a function of soil volumetric liquid water content (LWC) at the Montmorency Forest (MM) and Sodankylä (SOD–for) boreal forest uplands study sites, the only sites where liquid water was present during our winter campaigns. A linear regression was fitted for the SOD–for boreal forest uplands data and MM data, excluding the thick organic layer site. There is only one sampling location for the MM thick organic layer, whereas there are 9 sampling locations for the MM thin organic layer and 9 for the SOD–for. A polynomial regression was fitted to all data.

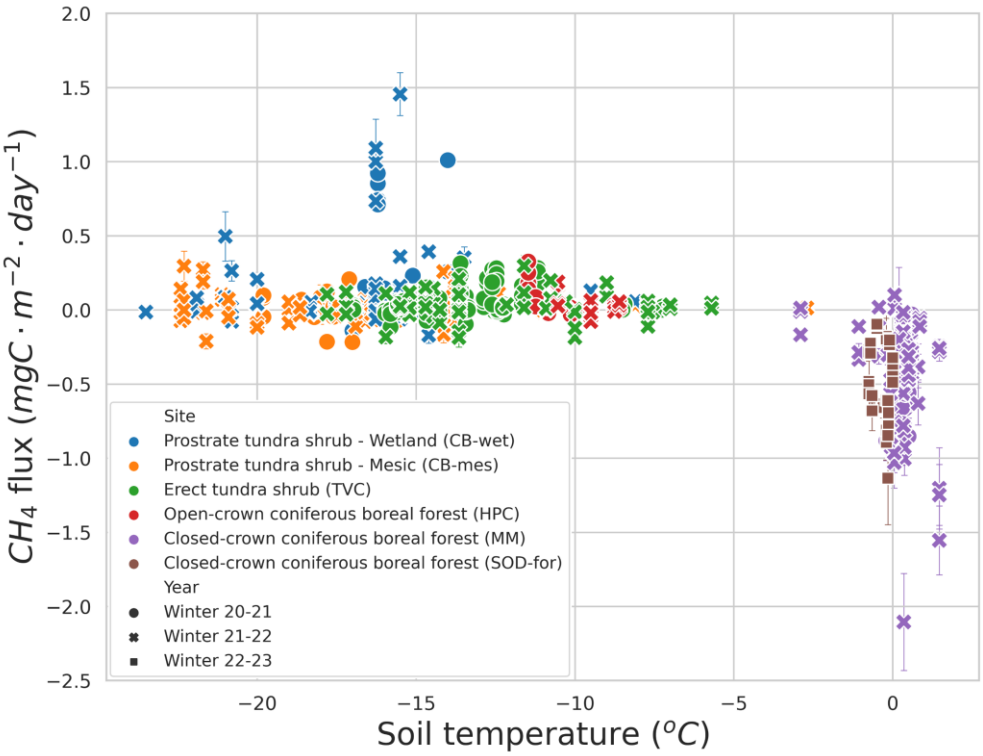

Figure 3. CH_4 flux as a function of soil temperature at 1 cm depth at the study sites of Cambridge Bay (CB), Trail Valley Creek (TVC), Havikpak Creek, Montmorency Forest (MM) during winter 2020–2021 and 2021–2022, and at Sodankylä (SOD–for).

4 Discussion

CH_4 flux regimes were previously observed mostly during the growing season, whereas our study focused on winter CH_4 fluxes. Our findings support the prevailing notion of boreal forest upland soils generally acting as CH_4 sinks (Lai, 2009; Lee et al., 2023) and wetlands acting as CH_4 sources (Oertel et al., 2016), and that these patterns hold true for the winter period. The winter CH_4 fluxes at the upland tundra sites were too low to classify these sites as either net sources or net sinks. The study sites with milder climates, MM and SOD, displayed the highest CH_4 fluxes, whether as CH_4 sink or source (Fig. 1). These sites have higher mean annual air temperatures (1.6 to 2.0 °C compared to –12.5 to –6.6 °C at CB, TVC, and HPC), no permafrost, longer growing seasons (94 to 113 days compared to 168 to 171 days at CB, TVC, and HPC), and higher annual precipitation (507 to 1293 mm compared to 152 to 198 mm at CB, TVC, and HPC). We also identified a few CH_4 emission hotspots in Arctic tundra wetlands during winter that emitted on average about 26 times more CH_4 than the average of other sample locations (0.78 vs. 0.03 mg C m^{-2} day^{-1}). All those CH_4 emission hotspots were found in wetland environments with high soil nutrient content (soil nutrient content determined from Ponomarenko et al., 2019). However, it is important to note that not all sampling locations in wetlands with high soil nutrient content exhibited CH_4 emission hotspots ($F_{CH4} \geq 0.35$ mg C m^{-2} day^{-1}); only 37.5% of wetland sampling locations exhibited high CH_4 emissions. Although we did not determine spatially integrated flux estimates for our sites, these hotspots may dominate the winter CH_4 flux budget.

Our results do not show a strong correlation between winter CH_4 fluxes and T_{soil} or snow parameters, unlike some previous studies that have found a correlation between CH_4 flux and sub–zero T_{soil} (Rößger et al., 2022). It is possible that surface T_{soil} at 1 cm depth in our study did not correlate with CH_4 fluxes, but that deeper T_{soil} could have a stronger correlation since most CH_4 production occurs in deeper soil layers (Henneron et al., 2022; Li et al., 2023). If further investigations show that deeper T_{soil} still does not correlate strongly with winter CH_4 fluxes in ABR, several terrestrial biosphere models would have to reassess how CH_4 fluxes are estimated as most use T_{soil} or T_{air} as a main control of CH_4 flux computation. However, it is also possible that other factors are masking the temperature dependency of winter CH4 fluxes, such as a strong inter–site variability of fluxes between the measurement locations at different land cover and vegetation types. According to Lee et al. (2023), soil organic carbon content has also been shown to be an important control on CH_4 sinks of forested regions which might be why the rate of CH_4 uptake increase with soil LWC is site–specific and the temperature dependence weak. We observed a weak correlation between F_{CH4} and F_{CO2} fluxes (measured in our previous study; Mavrovic et al., 2023) at the boreal forest upland sites (Fig. S5), which might be an indication of increased CH_4 uptake with higher soil carbon substrate availability or soil microbial activity as discovered recently for growing season CH_4 uptake (Voigt et al. 2023). The slower diffusion of CH_4 to the atmosphere in winter due to the fraction of soil pores filled with ice in frozen soils might also be contributing to masking the temperature dependency of winter CH_4 fluxes assuming again that an important fraction of CH_4 emissions occurs deeper than the measured soil temperature.

The boreal forest upland sites (MM and SOD–for) displayed a relatively strong correlation between F_{CH4} and soil LWC (R^2 = 0.21 and 0.73, respectively), although the rate of CH_4 uptake increases with soil LWC seemed to be site–specific. Despite differences in vegetation, soil, latitude, and precipitation, both sites displayed a similar range of net CH_4 uptake from the atmosphere. The main common characteristics between MM and SOD are the length of the growing season and the mean average air temperature (Table S2). MM and SOD are also the only study sites where the soil remained mostly unfrozen throughout winter. Unfrozen, well–drained soils have more pore space than frozen ones because of ice volume expansion. Larger pore space benefits CH_4 oxidation through increased diffusion rates (Ball et al., 1997; Smith et al., 2000). The MM and SOD–for sites also displayed a similar range of CO_2 emissions during winter, stressing that MM and SOD–for sites have comparable carbon flux regimes (Fig. S6; Mavrovic et al., 2023).

The SOD–wet boreal wetland CH_4 emissions were high but seemed to be limited by transport through the thick solid ice that formed in the wetland's upper layer. In April, during snowmelt, CH_4 concentrations under the 10–30 cm ice layer on top of the soil reached up to 1000 ppm at some sampling locations. The non–negligible F_{CH4} observed at the wetland indicates that the thick ice layer is porous but the underlying CH_4 production is higher than what is released into the atmosphere, at least for this part of winter. The trapped CH_4 is probably released during ice melt, which is coherent with previous studies that showed bursts of CH_4 emissions during spring melt (Song et al., 2012; Raz–Yaseef et al., 2016). Further investigation would be required to determine if the strong spatial variability observed in the boreal wetland is mainly due to variability in the upper ice layer porosity or variability in the underlying CH_4 production.

The shoulder seasons (i.e., autumn freeze and spring thaw) are important periods of change in CH_4 exchange regimes with an important contribution to the annual CH_4 budget (Arndt et al., 2020; Bao et al., 2021). Whereas this study presents results from the sites of MM, CB, and SOD–wet covering most of the winter with monthly flux measurement, the flux measurements of the study sites of TVC, HPC, and SOD–for covered only short winter campaigns (Table S2). Furthermore, the snowpack diffusive gradient method is limited to measurements within the snow–covered period. Further investigation of shoulder seasons CH_4 fluxes should be conducted to provide a better understanding of the inter–annual variability of the carbon cycle in ABR. Soil biogeochemical properties such as the quantity and quality of available carbon compounds were not addressed in this study but were shown to be important environmental controls of CH_4 fluxes (Aronson et al., 2013; Kharitonov et al., 2021; Lee et al., 2023; Voigt et al., 2023). Soil biogeochemical properties are generally strongly correlated with plant community composition and thus CH_4 flux (Bastviken et al., 2023). Biogeochemical analyses, as well as studies on microbial community composition and functioning during winter might help to explain the site–specific linear relationship between CH_4 flux and soil LWC, and, importantly, the lack of temperature dependence we observed in our study. Additionally, our study points towards the relevance of ice conditions in wetlands for understanding winter CH_4 fluxes and highlights the importance of an integrative view of CH_4 fluxes and soil properties.

5 Conclusions

We measured *in situ* winter CH_4 flux over five Arctic and boreal sites in Canada and Finland with diverse ecosystem types. Our findings indicate non–negligible winter F_{CH4}, which must be accounted for in annual carbon balance and terrestrial biosphere models over ABR. Although F_{CH4} of most Arctic sites was low, emission hotspots were observed in tundra and boreal wetlands. In the boreal forest uplands, soil liquid water content was identified as an important environmental control on net CH_4 uptake from the atmosphere, but the rate of CH_4 uptake increase with soil LWC dependency was different for the two boreal forest uplands study sites. It will be important to investigate if this site–specific LWC dependency could be related to other environmental controls such as soil physical–chemical properties and vegetation composition. The boreal wetland site displayed high CH_4 emissions throughout winter with high spatial variability, stressing the importance of further investigating the magnitude of these emissions from other sites and wetland ecotypes. Contrary to some other studies, we found a lack of temperature dependence on winter CH_4 flux across the different ABR ecosystems investigated, this is a significant finding that should be investigated further since several terrestrial biosphere models use soil temperature as a main control of winter CH_4 fluxes. Our study stresses the importance of considering ABR winter CH_4 flux to accurately calculate the carbon budget in these sensitive environments.

Acknowledgment

This work was made possible thanks to the contributions of the Natural Sciences and Engineering Research Council of Canada (NSERC), the Fonds de recherche du Québec – Nature et technologies (FRQNT) and Polar Knowledge Canada (POLAR). Carolina Voigt was supported by the BMBF project MOMENT (no. 03F0931A). A special thanks to people that contributed to data collection and gas analyzing: Milja Männikkö (Finnish Meteorological Institute [FMI]), Jaakko Nissilä (FMI), Anna Kontu (FMI), Marika Honkanen (FMI), Aleksi Rimali (FMI), Elmeri Viuho Hanne Suokanerva (FMI), Elise Imbeau (Viventem), Gabriel Ferland (Viventem), Aili Pedersen

(POLAR), Gabriel Hould Gosselin (Université de Montréal [UdeM] and Wilfrid Laurier University [WLU]), Rosy Tutton (WLU), Emma Riley (UdeM), Nick Rutter (Northumbria University [NU]), Paul Mann (NU), Victoria Dutch (NU), Georgina Woolley (NU), Élise Groulx (Université de Sherbrooke [UdeS]), Charlotte Crevier (UdeS), Érika Boisvert (UdeS), Alain Royer (UdeS), Patrick Ménard (UdeS), Vincent Sasseville (UdeS), Célia Trunz (UdeS), Daniel Kramer (UdeS), Estéban Hamel Jomphe (UQTR), Samuel Goulet (UQTR), Alex Gélinas (UQTR), David de Courville (UQTR), Juliette Ortet (UQTR) and Chris Derksen (Environment and Climate Change Canada). We would also like to thank Ian Hogg, Johann Wagner, and Scott Johnson from POLAR as well as Branden Walker and Philip Marsh from WLU for their logistical support.

Open Research

All data presented in this article can be found in the following repository:

Mavrovic, A., Sonnentag, O., Voigt, C., Roy, A. (2023). Winter CH4 fluxes over arctic and boreal environments. https://doi.org/10.5683/SP3/COWXAZ, Borealis.

References

Andresen, C., Lara, M., Tweedie, C., & Lougheed, V. (2017), Rising plant–mediated methane emissions from arctic wetlands. *Global Change Biology*, 23(3), 1128–1139, doi: 10.1111/gcb.13469

Arndt, K., Lipson, D., Hashemi, J., Oechel, W., & Zona, D. (2020), Snow melt stimulates ecosystem respiration in Arctic ecosystems. *Global Change Biology*, 26(9), 5042–5051, doi: 10.1111/gcb.15193

Aronson, E., Allison, S., & Helliker, B. (2013), Environmental impacts on the diversity of methane–cycling microbes and their resultant function. *Frontiers in Microbiology*, 4, 225, doi: 10.3389/fmicb.2013.00225

Ball, B., Smith, K., Klemedtsson, L., Brumme, R., Sitaula, B., Hansen, S., Priemé, A., MacDonald, J., & Horgan, G. (1997), The influence of soil gas transport properties on methane oxidation in a selection of northern European soils. *Journal of Geophysical Research: Atmospheres*, 102(D19), 23309–23317, doi: 10.1029/97JD01663

Bao, T., Xu, X., Jia, G., Billesbach, D., & Sullivan, R. (2020), Much stronger tundra methane emissions during autumn-freeze than spring-thaw. *Global Change Biology*, 27(2), 376–387, doi: 10.1111/gcb.15421

Barry R, Plamondon, AP, & Stein, J. (1988), Hydrologic soil properties and application of a soil moisture model in a balsam fir forest. *Canadian Journal of Forest Research*, 18(4), 427– 434, doi: 10.1139/x88–063

Bastviken, D., Treat, C., Pangala, S. R., Gauci, V., Enrich–Prast, A., Karlson, M., Gålfalk, M., Romano, B., Sawakuchi, H. O. (2023), The importance of plants for methane emission at the ecosystem scale. *Aquatic Botany*, 184, 103596, doi: 10.1016/j.aquabot.2022.103596

Bekryaev, R. V., Polyakov, I. V., & Alexeev, V. A. (2010), Role of polar amplification in long–term surface air temperature variations and modern arctic warming. *Journal of Climate*, 23(14), 3888–3906, doi:10.1175/2010jcli3297.1

Bowley, A. (1928), The standard deviation of the correlation coefficient. *Journal of the American Statistical Association*, 23(161), 31–34, doi:10.2307/2277400

Brown, J., Ferrians, O., Heginbottom, J., & Melnikov, E (2002), Circum–Arctic map of permafrost and ground–ice conditions, Version 2. Boulder, Colorado, USA, NSIDC: National Snow and Ice Data Center, doi: 10.7265/skbg–kf16

Dean, J., Middelburg, J., Röckmann, T., Aerts, R., Blauw, L. G., Egger, M., Jetten, M., de Jong, A., Meisel, O., Rasigraf, O., Slomp, C., in't Zandt, M., & Dolman, A. (2018), Methane feedbacks to the global climate system in a warmer world. *Reviews of Geophysics*, 56(1), 207–250. doi:10.1002/2017rg000559

Deluca, T., & Boisvenue, C. (2012), Boreal forest soil carbon: distribution, function and modelling. *Forestry*, 85(2), 161–184, doi: 10.1093/forestry/cps003

Delwiche, K., Knox, S., Malhotra, A., Fluet–Chouinard, E., McNicol, G., Feron, S., Ouyang, Z., Papale, D., Trotta, C., Canfora, E., Cheah, Y.–W., Christianson, D., Alberto, M. C., Alekseychik, P., Aurela, M., Baldocchi, D., Bansal, S., Billesbach, D., Bohrer, G., Bracho, R., Buchmann, N., Campbell, D., Celis, G., Chen, J., Chen, W., Chu, H., Dalmagro, H., Dengel, S., Desai, A., Detto, M., Dolman, H., Eichelmann, E., Euskirchen, E., Famulari, D., Fuchs, K., Goeckede, M., Gogo, S., Gondwe, M., Goodrich, J., Gottschalk, P., Graham, S., Heimann, M., Helbig, M., Helfter, C., Hemes, K., Hirano, T., Hollinger, D., Hörtnagl, L., Iwata, H., Jacotot, A., Jurasinski, G., Kang, M., Kasak, K., King, J., Klatt, J., Koebsch, F., Krauss, K., Lai, D., Lohila, A., Mammarella, I., Marchesini, L. B., Manca, G., Matthes, J. H., Maximov, T., Merbold, L., Mitra, B., Morin, T., Nemitz, E., Nilsson, M., Niu, S., Oechel, W., Oikawa, P., Ono, K., Peichl, M., Peltola, O., Reba, M., Richardson, A., Riley, W., Runkle, B., Ryu, Y., Sachs, T., Sakabe, A., Sanchez, C., Schuur, E., Schäfer, K., Sonnentag, O., Sparks, J., Stuart–Haëntjens, E., Sturtevant, C., Sullivan, R., Szutu, D., Thom, J., Torn, M., Tuittila, E.–S., Turner, J., Ueyama, M., Valach, A., Vargas, R., Varlagin, A., Vazquez–Lule, A., Verfaillie, J., Vesala, T., Vourlitis, G., Ward, E., Wille, C., Wohlfahrt, G., Wong, G., Zhang, Z., Zona, D., Windham–Myers, L., Poulter, B., & Jackson, R. (2021), FLUXNET–CH4: a global, multi–ecosystem dataset and analysis of methane seasonality from freshwater wetlands. *Earth System Science Data*, 13(7), 3607–3689, doi: 10.5194/essd–13–3607–2021

Derksen, C., Burgess, D., Duguay, C., Howell, S., Mudryk, L., Smith, S., Thackeray, C., & Kirchmeier–Young, M. (2019), Changes in snow, ice, and permafrost across Canada. Canada's Changing Climate Report – Chapter 5, Government of Canada, Ottawa, Ontario, Canada, 194–260.

Du Plessis, J. P., Masliyah, J. H. (1991), Flow through isotropic granular porous media. *Transport in Porous Media*, 6, 207–221, doi: 10.1007/BF00208950

Fierz, C., A., Durand, Y., Etchevers, P., Green, E., McClung, D., Nishimura, K., Satyawali, P., & Sokratov, S. (2009), The international classification for seasonal snow on the ground, IHP–VII Technical Documents in Hydrology N83, IACS Contribution N1, UNESCO–IHP, Paris.

Fisher, J., Sikka, M., Oechel, W., Huntzinger, D., Melton, J., Koven, C., Ahlström, A., Arain, M., Baker, I., Chen, J., Ciais, P., Davidson, C., Dietze, M., El–Masri, B., Hayes, D., Huntingford, C., Jain, A., Levy, P., Lomas, R., Poulter, B., Price, D., Sahoo, A., Schaefer, K., Tian, H., Tomelleri, E., Verbeeck, H., Viovy, N., Wania, R., Zeng, N., & Miller, C. (2014), Carbon cycle uncertainty in the Alaskan Arctic. *Biogeosciences*, 11(15), 4271–4288, doi: 10.5194/bg–11–4271–2014

Fooladmand, H. R. (2011), Estimating soil specific surface area using the summation of the number of spherical particles and geometric mean particle–size diameter. African Journal of Agricultural Research, 6(7), 1758–1762, doi: 10.5897/AJAR11.19

Grünberg, I., Wilcox, E., Zwieback, S., Marsh, P., & Boike, J. (2020), Linking tundra vegetation, snow, soil temperature, and permafrost. *Biogeosciences*, 17(16), 4261–4279. doi: 10.5194/bg–17–4261–2020

Harvey, A., In Haynes, W., Lide, D., & Bruno, T. (2017), CRC Handbook of Chemistry and Physics (97th ed.): Properties of Ice and Supercooled Water. CRC Press, Boca Raton, Florida, United States, 2666 pages (6–12). ISBN 978–1–4987–5429–3

Helbig, M., Chasmer, L. E., Kljun, N., Quinton, W. L., Treat, C. C., & Sonnentag, O. (2016), The positive net radiative greenhouse gas forcing of increasing methane emissions from a thawing boreal forest–wetland landscape. *Global Change Biology*, 23(6), 2413–2427, doi:10.1111/gcb.13520

Henneron, L., Balesdent, J., Alvarez, G., Barré, P., Baudin, F., Basile–Doelsch, I., Cécillon, L., Fernandez–Martinez, A., Hatté, C., & Fontaine, S. (2022), Bioenergetic control of soil carbon dynamics across depth. *Nature Communications*, 13, 7676, doi: 10.1038/s41467–022–34951–w

Hiyama, T., Ueyama, M., Kotani, A., Iwata, H., Nakai, T., Okamura, M., Ohta, T., Harazono, Y., Petrov, R.E., & Maximov, T.C. (2020), Lessons learned from more than a decade of greenhouse gas flux measurements at boreal forests in eastern Siberia and interior Alaska, *Polar Science*, 27, 100607, doi: 10.1016/j.polar.2020.100607

Ikonen, J., Vehviläinen, J., Rautiainen, K., Smolander, T., Lemmetyinen, J., Bircher, S., & Pulliainen, J. (2016), The Sodankylä in situ soil moisture observation network: an example application of ESA CCI soil moisture product evaluation. *Geoscientific Instrumentation, Methods and Data Systems*, 5, 95–108, doi:10.5194/gi–5–95–2016

Ito, A., Li, T., Qin, Z., Melton, J., Tian, H., Kleinen, T., Zhang, W., Zhang, Z., Joos, F., Ciais, P., Hopcroft, P., Beerling, D., Liu, X., Zhuang, Q., Zhu, Q., Peng, C., Chang, K.–Y., Fluet–Chouinard, E., McNicol, G., Patra, P., Poulter, B., Sitch, S., Riley, W., & Zhu, Q. (2023), Cold–season Methane fluxes simulated by GCP–CH4 models. *Geophysical Research Letters*, 50(14), e2023GL103037, doi: 10.1029/2023GL103037

Kharitonov, S., Semenov, M., Sabrekov, A., Kotsyurbenko, O., Zhelezova, A., & Schegolkova, N. (2021), Microbial communities in methane cycle: modern molecular methods gain insights into their global ecology. *Environments*, 8(2), 16, doi: 10.3390/environments8020016

Kibtia, H., Abdullah, S., & Bustamam, A. (2020), Comparison of random forest and support vector machine for prediction of cognitive impairment in Parkinson's disease. *AIP Conference Proceedings*, 2296(1), 020093. doi: 10.1063/5.0030332

Kim, Y., Ueyama, M., Nakagawa, F., Tsunogai, U., Harazono, Y., & Tanaka, N. (2007), Assessment of winter fluxes of CO_2 and CH_4 in boreal forest soils of central Alaska estimated by the profile method and the chamber method: a diagnosis of methane emission and implications for the regional carbon budget. *Tellus B: Chemical and Physical Meteorology*, 59(2), 223–233, doi: 10.1111/j.1600–0889.2006.00233.x

Kim, Y., Tsunogai, S., & Tanaka, N. (2019), Winter CO_2 emission and its production rate in cold temperate soils of northern Japan: 222Rn as a proxy for the validation of CO_2 diffusivity. *Polar Science*, 22, 100480, doi: 10.1016/j.polar.2019.09.002

Kinar, N., & Pomeroy, J. (2015), Measurement of the physical properties of the snowpack. *Reviews of Geophysics*, 53(2), 481–544, doi: 10.1002/2015RG000481

King, J., Reeburgh, W., & Regli, S. K. (1998), Methane emission and transport by arctic sedges in Alaska: Results of a vegetation removal experiment. *Journal of Geophysical Research: Atmospheres*, 103(D22), 29083–29092, doi:10.1029/98jd00052

Kirschke, S., Bousquet, P., Ciais, P., Saunois, M., Canadell, J., Dlugokencky, E., Bergamaschi, P., Bergmann, D. Blake, D., Bruhwiler, L., Cameron–Smith, P., Castaldi, S., Chevallier, F., Feng, L., Fraser, A., Heimann, M., Hodson, E., Houweling, S., Josse, B., Fraser, P., Krummel, P., Lamarque, J.–F., Langenfelds, R., Le Quéré, C., Naik, V., O'Doherty, S., Palmer, P., Pison, I., Plummer, D., Poulter, B., Prinn, R., Rigby, M., Ringeval, B., Santini, M., Schmidt, M., Shindell, D., Simpson, I., Spahni, R., Steele, L. P., Strode, S., Sudo, K., Szopa, S., van der Werf, G., Voulgarakis, A., van Weele, M., Weiss, R., Williams, J., & Zeng, G. (2013), Three decades of global methane sources and sinks. *Nature Geoscience*, 6(10), 813–823, doi:10.1038/ngeo1955

Knox, S., Jackson, R., Poulter, B., McNicol, G., Fluet–Chouinard, E., Zhang, Z., Hugelius, G., Bousquet, P., Canadell, J., Saunois, M., Papale, D., Chu, H., Keenan, T., Baldocchi, D., Torn, M., Mammarella, I., Trotta, C., Aurela, M., Bohrer, G., Campbell, D., Cescatti, A., Chamberlain, S., Chen, J., Chen, W., Dengel, S., Desai, A., Euskirchen, E., Friborg, T., Gasbarra, D., Goded, I., Goeckede, M., Heimann, M., Helbig, M., Hirano, T., Hollinger, D., Iwata, H., Kang, M., Klatt, J., Krauss, K., Kutzbach, L., Lohila, A., Mitra, B., Morin, T., Nilsson, M., Niu, S., Noormets, A., Oechel, W., Peichl, M., Peltola, O., Reba, M., Richardson, A., Runkle, B., Ryu, Y., Sachs, T., Schäfer, K., Schmid, H. P., Shurpali, N., Sonnentag, O., Tang, A., Ueyama, M., Vargas, R., Vesala, T., Ward, E., Windham–Myers, L., Wohlfahrt, G., & Zona, D. (2019), FLUXNET–CH4 synthesis activity: objectives, observations, and future directions. *Bulletin of the American Meteorological Society*, 100(12), 2607–2632, doi:10.1175/bams–d–18–0268.1

Krogh, S., Pomeroy, J., & Marsh, P. (2017), Diagnosis of the hydrology of a small Arctic basin at the tundra–taiga transition using a physically based hydrological model. *Journal of Hydrology*, 550, 685–703, doi: 10.1016/j.jhydrol.2017.05.042

Kuhn, M. A., Varner, R. K., Bastviken, D., Crill, P., MacIntyre, S., Turetsky, M., Walter Anthony, K., McGuire, A. D., & Olefeldt, D. (2021), BAWLD–CH_4: a comprehensive dataset of methane fluxes from boreal and arctic ecosystems. *Earth System Science Data*, 13, 5151–5189, doi: 10.5194/essd–13–5151–2021

Lai, D. (2009), Methane dynamics in northern peatlands: A Review. *Pedosphere*, 19(4), 409–421, doi: 10.1016/S1002–0160(09)00003–4

Lee, J., Oh, Y., Lee, S. T., Seo, Y. O., Yun, J., Yang, Y., Kim, J., Zhuang, Q., & Kang, H. (2023), Soil organic carbon is a key determinant of CH4 sink in global forest soils. *Nature Communications*, 14, 3110, doi: 10.1038/s41467–023–38905–8

Li, K., Wang, Z., Xiang, Q., Zhao, X., Ji, L., Xin, Y., Sun, J., Liu, C., Shen, X., Xu, X., & Chen, Q. (2023), Coupling of soil methane emissions at different depths under typical coastal wetland vegetation types. *Chemosphere*, 338, 139505, doi: 10.1016/j.chemosphere.2023.139505

Liaw, A., & Wiener, M. (2002), Classification and regression by RandomForest. *R News*, 2(3), 18–22.

Madore, J.–B., Fierz, C., & Langlois, A. (2022), Investigation into percolation and liquid water content in a multi–layered snow model for wet snow instabilities in Glacier National Park, Canada. *Frontiers in Earth Science*, 10, 898980, doi: 10.3389/feart.2022.898980

Marrero, T., & Mason E. (1972), Gaseous diffusion coeffcients. *Journal of Physics and Chemistry Reference Data*, 1(1), 3–117, doi: 10.1063/1.3253094

Martin, M., Kumar, P., Sonnentag, O., & Marsh, P. (2022), Thermodynamic basis for the demarcation of Arctic and alpine treelines. *Scientific Reports*, 12, 12565, doi: 10.1038/s41598–022–16462–2

Massman, W. (1998), A review of the molecular diffusivities of H_2O, CO_2, CH_4, CO, O_3, SO_2, NH_3, N_2O, NO, and NO_2 in air, O_2 and N_2 near STP. *Atmospheric Environment*, 32(6), 1111–1127, doi: 10.1016/S1352–2310(97)00391–9

Mastepanov M, Sigsgaard, C., Tagesson, T., Ström, L., Tamstorf, M., Lund, M., & Christensen, T. (2013), Revisiting factors controlling methane emissions from high–Arctic tundra. *Biogeosciences*, 10(7), 5139–5158, doi: 10.5194/bg–10–5139–2013

Mavrovic, A., Sonnentag, O., Lemmetyinen, J., Voigt, C., Rutter, N., Mann, P., Sylvain, J.–D., Roy, A. (2023), Environmental controls of winter soil carbon dioxide fluxes in boreal and tundra environments. *Biogeosciences*, 20(24), 5087–5108, doi: 10.5194/bg-20-5087-2023

McDowell, N., Marshall, J., Hooker, T., & Musselman, R. (1999), Estimating CO_2 flux from snowpacks at three sites in the Rocky Mountains. *Tree physiology*, 20, 745–753, doi: 10.1093/treephys/20.11.745

McGuire, A., Christensen, T., Hayes, D., Heroult, A., Euskirchen, E., Kimball, J., Koven, C., Lafleur, P., Miller, P., Oechel, W., Peylin, P., Williams, M., & Yi, Y. (2012), An assessment of the carbon balance of Arctic tundra: Comparisons among observations, process models, and atmospheric inversions. *Biogeosciences*, 9(8), 3185–3204, doi: 10.5194/bg–9–3185–2012

Natali S., Holdren, J., Rogers, B., Treharne, R., Duffy, P., Pomerance, R., & MacDonald, E. (2021), Permafrost carbon feedbacks threaten global climate goals. *Proceedings of the National Academy of Sciences*, 118(21), e2100163118, doi: 10.1073/pnas.2100163118

Oertel, C., Matschullat, J., Zurba, K., Zimmermann, F., & Erasmi, S. (2016), Greenhouse gas emissions from soils – A review. *Geochemistry*, 76(3), 327–352, doi: 10.1016/j.chemer.2016.04.002

Pirk, N., Tamstorf, M., Lund, M., Mastepanov, M., Pedersen, S., Myllus, M., Parmentier, F.–J., Christiansen, H., & Christensen (2016), Snowpack fluxes of methane and carbon dioxide from high Arctic tundra. *Biogeosciences*, 121(11), 2886–2900, doi: 10.1002/2016JG003486

Potapov, P., Hansen, M., Stehman, S., Loveland, T., & Pittman, K. (2008), Combining MODIS and Landsat imagery to estimate and map boreal forest cover loss. *Remote Sensing of Environment*, 112(9), 3708–3719, doi: 10.1016/j.rse.2008.05.006

Proksch, M., Rutter, N., Fierz, C., & Schneebeli, M. (2016), Intercomparison of snow density measurements: bias, precision, and vertical resolution. *The Cryosphere*, 10(1), 371–384, doi: 10.5194/tc–10–371–2016.

Rantanen, M., Karpechko, A.Y., Lipponen, A., Nordling, K., Hyvärinen, O., Ruosteenoja, K., Vihma, T. & Laaksonen, A. (2022), The Arctic has warmed nearly four times faster than the globe since 1979. *Communications Earth & Environment*, 3(1), 1–10, doi: 10.1038/s43247–022–00498–3.

Ravn, N., Elberling, B., & Michelsen, A. (2020), Arctic soil carbon turnover controlled by experimental snow addition, summer warming and shrub removal. *Soil Biology and Biochemistry*, 142, 107698, doi: 10.1016/j.soilbio.2019.107698

Raz–Yaseef, N., Torn, M., Wu, Y., Billesbach, D., Liljedahl, A., Kneafsey, T., Romanovsky, V., Cook, D., & Wullschleger, S. (2016), Large CO_2 and CH_4 emissions from polygonal tundra during spring thaw in northern Alaska. *Geophysical Research Letters*, 44(1), 504–513, doi: 10.1002/2016GL071220

Roslev, P., Iversen, N., & Henriksen, K. (1997), Oxidation and assimilation of atmospheric methane by soil methane oxidizers. *Applied and Environmental Microbiology*, 63(3), 874–880, doi: 10.1128/aem.63.3.874–880.1997

Rößger, N., Sachs, T., Wille, C., Boike, J., & Kutzbach, L. (2022), Seasonal increase of methane emissions linked to warming in Siberian tundra. *Nature Climate Change*, 12(11), 1031–1036, doi: 10.1038/s41558–022–01512–4

Schuur, E., McGuire, A., Schädel, C., Grosse, G., Harden, J., Hayes, D., Hugelius, G., Koven, C., Kuhry, P., Lawrence, D., Natali, S., Olefeldt, D., Romanovsky, V., Schaefer, K., Turetsky, M., Treat, C., & Vonk, J. (2015), Climate change and the permafrost carbon feedback. *Nature*, 520, 171–179, doi: 10.1038/nature14338

Schuur, E., Abbott, B., Commane, R., Ernakovich, J., Euskirchen, E., Hugelius, G., Grosse, G., Jones, M., Koven, C., Leshyk, V., Lawrence, D., Loranty, M., Mauritz, M., Olefeldt, D., Natali, S., Rodenhizer, H., Salmon, V., Schädel, C., Strauss, J., Treat, C., & Turetsky, M. (2022), Permafrost and climate change: carbon cycle feedbacks from the warming Arctic. *Annual Review of Environment and Resources*, 47(1), 343–371, doi: 10.1146/annurev–environ–012220–011847

Seok, B., Helmig, D., Williams, M., Liptzin, D., Chowanski, K., & Hueber, J. (2009), An automated system for continuous measurements of trace gas fluxes through snow: an evaluation of the gas diffusion method at a subalpine forest site, Niwot Ridge, Colorado. *Biogeochemistry*, 95, 95–113, doi: 10.1007/s10533–009–9302–3

Smith, K., Dobbie, K., Ball, B., Bakken, L., Sitaula, B., Hansen, S., Brumme, R., Borken, W., Christensen, S., Priemé, A., Fowler, D., Macdonald, J., Skiba, U., Klemedtsson, L., Kasimir–Klemedtsson, A., Degórska, A., & Orlanski, P. (2000), Oxidation of atmospheric methane in Northern European soils, comparison with other ecosystems, and uncertainties in the global terrestrial sink. *Global Change Biology*, 6(7), 791–803, doi: 10.1046/j.1365–2486.2000.00356.x

Sommerfeld, R., Mosier, A., & Musselman, R. (1993), CO_2, CH_4 and N_2O flux through a Wyoming snowpack and implications for global budgets. *Nature*, 361, 140–142, doi: 10.1038/361140a0

Song, C., Xu, X., Sun, X., Tian, H., Sun, L., Miao, Y., Wang, X., & Guo, Y. (2012), Large methane emission upon spring thaw from natural wetlands in the northern permafrost region. *Environmental Research Letters*, 7(3), 034009, doi: 10.1088/1748–9326/7/3/034009

Tanja, S., Berninger, F., Vesala, T., Markkanen, T., Hari, P., Mäkelä, A., Ilvesniemi, H., Hänninen, H., Nikinmaa, E., Huttula, T., Laurila, T., Aurela, M., Grelle, A., Lindroth, A., Arneth, A., Shibistova, O., & Lloyd, J. (2003), Air temperature triggers the recovery of evergreen boreal forest photosynthesis in spring. *Global Change Biology*, 9(10), 1410–1426, doi: 10.1046/j.1365–2486.2003.00597.x

Tarnocai, C., Canadell, J., Schuur, E., Kuhry, P., Mazhitova, G., & Zimov, S. (2009), Soil organic carbon pools in the northern circumpolar permafrost region. *Global Biogeochemical Cycles*, 23(2), GB2023, doi: 10.1029/2008GB003327

Topp, E., & Pattey, E. (1997), Soils as sources and sinks for atmospheric methane. *Canadian Journal of Soil Science*, 77(2), 167–177, doi: 10.4141/S96–107

Treat, C. C., Bloom, A. A., & Marushchak, M. E. (2018), Nongrowing season methane fluxes – a significant component of annual fluxes across northern ecosystems. *Global Change Biology*, 24, 3331–3343, doi: 10.1111/gcb.14137

Ullah, S., Frasier, R., Pelletier, L., & Moore, T., (2009), Greenhouse gas fluxes from boreal forest soils during the snow–free period in Quebec, Canada. *Canadian Journal of Forest Research*, 39(3), 666–680, doi: 10.1139/X08–209

Virtanen, T., & Ek, M. (2014), The fragmented nature of tundra landscape. *International Journal of Applied Earth Observation*, 27(A), 4–12, doi: 10.1016/j.jag.2013.05.010

Viru, B., Veber, G., Jaagus, J., Kull, A., Maddison, M., Muhel, M., Espenberg, M., Teemusk, A., & Mander, Ü. (2020), Wintertime greenhouse gas fluxes in hemiboreal drained peatlands. *Atmosphere*, 11, 731, doi: 10.3390/atmos11070731

Voigt, C., Lamprecht, R., Marushchak, M., Lind, S., Novakovskiy, A., Aurela, M., Martikainen, P., & Biasi, C. (2017), Warming of subarctic tundra increases emissions of all three important greenhouse gases – carbon dioxide, methane, and nitrous oxide. *Global Change Biology*, 23(8), 3121–3138, doi: 10.1111/gcb.13563

Voigt, C., Virkkala, A.–M., Hould Gosselin, G., Bennett, K., Black, T. A., Detto, M., Chevrier–Dion, C., Guggenberger, G., Hashmi, W., Kohl, L., Kou, D., Marquis, C., Marsh, P., Marushchak, M., Nesic, Z., Nykänen, H., Saarela, T., Sauheitl, L., Walker, B., Weiss, N., Wilcox, E., & Sonnentag, O. (2023) Arctic soil methane sink increases with drier conditions and higher ecosystem respiration. *Nature Climate Change*, 13, 1095–1104, doi: 10.1038/s41558–023–01785–3

Yvon–Durocher, G., Allen, A., Bastviken, D., Conrad, R., Gudasz, C., St–Pierre, A., Thanh–Duc, N., & del Giorgio, P. A. (2014), Methane fluxes show consistent temperature dependence across microbial to ecosystem scales. *Nature*, 507(7493), 488–491, doi:10.1038/nature13164

Zhang, L., Zhao, T., Jiang, L., & Zhao, K. (2010), Estimate of phase transition water content in freeze–thaw process using microwave radiometer. *IEEE Transactions on Geoscience and Remote Sensing*, 48(12), 4248–4255, doi: 10.1109/TGRS.2010.2051158

Zhang, Z., Zimmermann, N., Stenke, A., Li, X., Hodson, E., Zhu, G., Huang, C., & Poulter, B. (2017), Emerging role of wetland methane emissions in driving 21st century climate change. *Proceedings of the National Academy of Sciences*, 114(36), 9647–9652, doi:10.1073/pnas.1618765114

Zhu, C., Nakayama, M., & Inouey, H. Y. (2014), Continuous measurement of CO_2 flux through the snowpack in a dwarf bamboo ecosystem on Rishiri Island, Hokkaido, Japan. *Polar Science*, 8(3), 218–231, doi: 10.1016/j.polar.2014.04.003

Zona, D., Oechel, W., Kochendorfer, J., Paw U, K., Salyuk, A., Olivas, P., Oberbauer, S., & Lipson, D. (2009), Methane fluxes during the initiation of a large–scale water table manipulation experiment in the Alaskan Arctic tundra. *Global Biogeochemical Cycles*, 23(2), GB2013, doi:10.1029/2009GB003487

Zona, D., Giolo, B., Commane, R., Lindaas, J., Wofsy, S., Miller, C., Dinardo, S., Dengel, S., Sweeney, C., Karion, A., Chang, R., Henderson, J., Murphy, P., Goodrich, J., Moreaux, V., Liljedahl, A., Watts, J., Kimball, J., Lipson, D., & Oechel, W. (2015), Cold season emissions dominate the Arctic tundra methane budget. *Proceedings of the National Academy of Sciences*, 113(1), 40–45, doi: 10.1073/pnas.1516017113

Supporting Information

Study sites

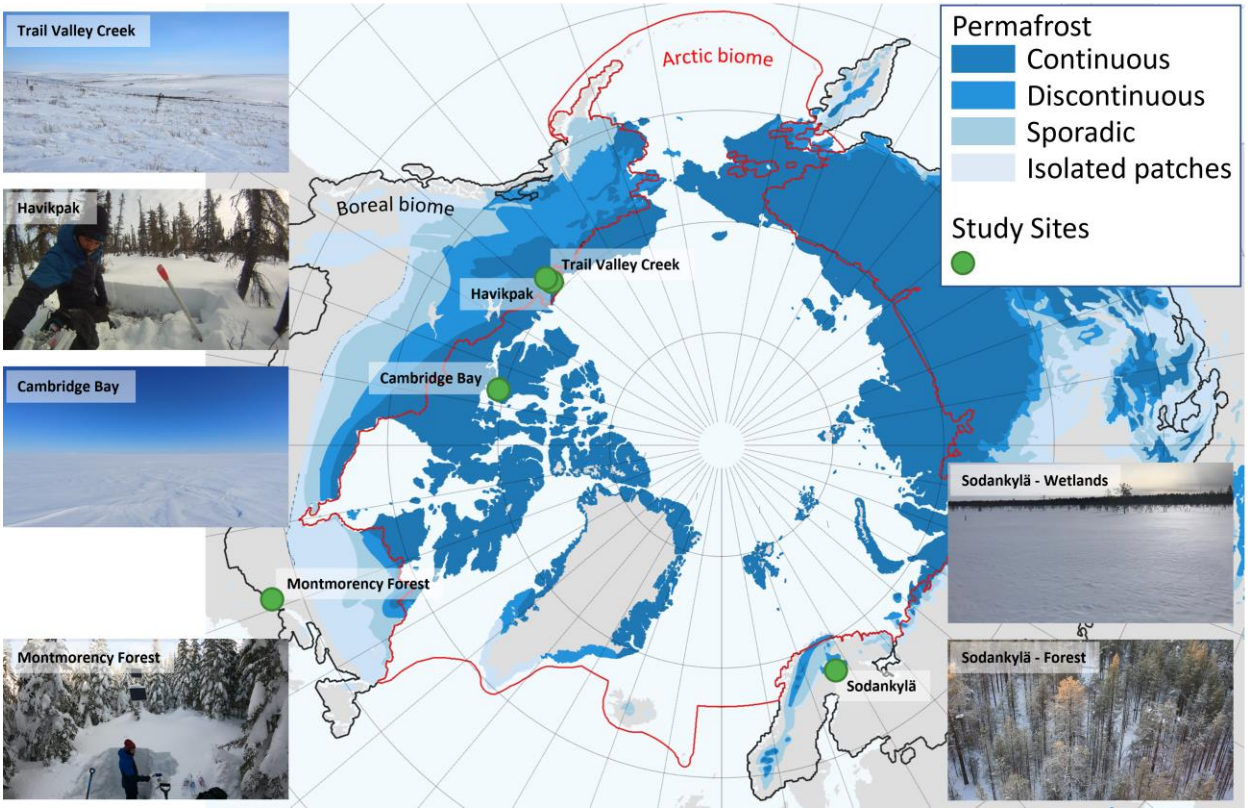

Figure S1. Study site locations. The Arctic biome is delimited following the Conservation of Arctic Flora and Fauna (CAFF) working group of the Arctic Council (Arctic SDI Catalogue, Identifier: 2ad7a7cb–2ad7–4517–a26e–7878ef134239, 2017) and the boreal biome is delimited following Potapov et al. (2008). Permafrost extent (Brown et al., 2002) is estimated in percent area: continuous (>90–100%), discontinuous (>50–90%), sporadic (>10–50%) and isolated patches (≤10%). Figure modified from Mavrovic et al. (2023).

Table S1. Study sites with the number of sampling locations and CH_4 flux measurement (N) for each site. Some study sites have more sampling locations than others because there were more vegetation types and a larger area to cover. Overall, every type of vegetation had 5–10 sampling locations. Table modified from Mavrovic et al. (2023).

Site	Acronym	Location	Latitude/ longitude	Sampling locations	N	Measurement months	Site reference
Cambridge Bay	CB	Nunavut, Canada	69°13'N 104°54'W	47	230	2021: 04, 12 2022: 01-05	Ponomarenko et al., 2019
Trail Valley Creek	TVC	Northwest Territories, Canada	68°46'N 133°28'W	34	152	2021: 03, 12 2022: 03	Grünberg et al., 2020
Havikpak Creek	HPC	Northwest Territories, Canada	68°19'N 133°31'W	5	30	2021: 03, 04 2022: 03	Krogh et al., 2017
Montmorency Forest	MM	Quebec, Canada	47°18'N 71°10'W	12	110	2021: 01, 02, 12 2022: 01-05	Barry et al., 1988
Sodankylä	SOD	Lapland, Finland	67°22'N 26°38'E	30	138	2022: 02-04 2022-2023: 12-05	Ikonen et al., 2016

Table S2. Vegetation, soil, and climate properties of the study sites. Mean annual air temperature, annual precipitation, and growing season length were evaluated for the years with CH_4 flux measurements (2021–2022 for CB, TVC, HPC and MM; 2022 for SOD). Growing season length was estimated from the last to the first day of frost using a 5–day running–average daily mean air temperature (Tanja et al., 2003).

Site	Ecosystem	Dominant specie	Acronym	Soil layers	Mean Annual T_{air}	Annual Precipitation	Growing Season Length	Permafrost
Cambridge Bay	Prostrate tundra shrubs	Lichen and moss	CB-mes	Mesic: 0-5 cm organic over dry mineral	-12.5 °C	152 mm	94 days	Continuous
	Open wetland	Sedge fen	CB-wet	Wetland: 10-20 cm organic over wet mineral (clay)				
Trail Valley Creek	Erect tundra shrubs	Schurb, lichen, moss and tussock	TVC	30-60 cm organic (peat) over mineral	-7.8 °C	175 mm	111 days	Continuous
Havikpak Creek	Open-crown coniferous boreal forest	Black spruce	HPC	5-50 cm organic (peat) over mineral (silty clay)	-6.6 °C	198 mm	113 days	Continuous
Montmorency Forest	Closed-crown coniferous boreal forest	Balsam fir	MM	4-7 cm litter over 7-13 cm organic over wet mineral (sandy loam)	2.0 °C	1293 mm	171 days	Absent
Sodankylä	Closed-crown coniferous boreal forest	Scots pine	SOD-for	0-5 cm organic over dry mineral (sand)	1.6 °C	507 mm	168 days	Absent
	Open wetland	Fen and bog	SOD-wet	> 120 cm organic (peatland)				

CH_4 flux uncertainty assessment

Sources of uncertainties for F_{CH4} can be subdivided into four categories: gas concentration estimates, gas transfer/transport/storage, snow properties estimates and $d[CH_4]/dz$ estimates. The uncertainty on $[CH_4]$ was evaluated from the gas analyzer precision as assessed by the manufacturer. $[CH_4]$ uncertainty was further tested using calibration gases. The gas transfer, transport and storage protocols were tested using calibration gases. The $d[CH_4]/dz$ linear regression uncertainties were evaluated using the standard deviation from the Pearson correlation coefficient ($\sigma = \sqrt{(1-R^2)/(N-1)}$; Bowley, 1928). F_{CH4} uncertainty was calculated by uncertainty propagation from $d[CH_4]/dz$ and snow density uncertainties.

The F_{CH4} uncertainty assessment showed that the two main sources of uncertainty are associated with snow density measurements ($\sigma(\rho_{snow}) \approx 9\%$); Proksch et al., 2016) and with $d[CH_4]/dz$ (mean $R^2 = 0.901$ ($\sigma = 0.135$) for $F_{CH4} \geq 0.05$ mg C m^{-2} day^{-1}; N = 339) (Table S1). The mean F_{CH4} uncertainty can be estimated at 16.89% for data from CB, TVC, MM and SOD–for boreal forest, and 3.76% for data from SOD–wet boreal wetland (Fig. S1).

Table S3. F_{CH4} uncertainty sources. $[CH_4]$ precision was evaluated at a concentration of 2 ppm.

F_{CH4} uncertainty source	Uncertainty
$[CH_4]$ estimate	
· LI-7810 precision	0.6 ppm (0.03%)
· Measurement stability	0.001 ppm (0.05%; N=169)
· Reference gas	0.018 ppm (1%)
· Calibration fit	0.005 ppm (0.25%; N=8; σ = 0.067%)
· Transfer, transport and storage test	0.012 ppm (0.63%; N=5)
Snow density ($kg \cdot m^{-3}$)	9%
$d[CH_4]/dz$ linear regression ($gC \cdot m^{-4}$)	17.66% (N=339; σ = 17.14%)

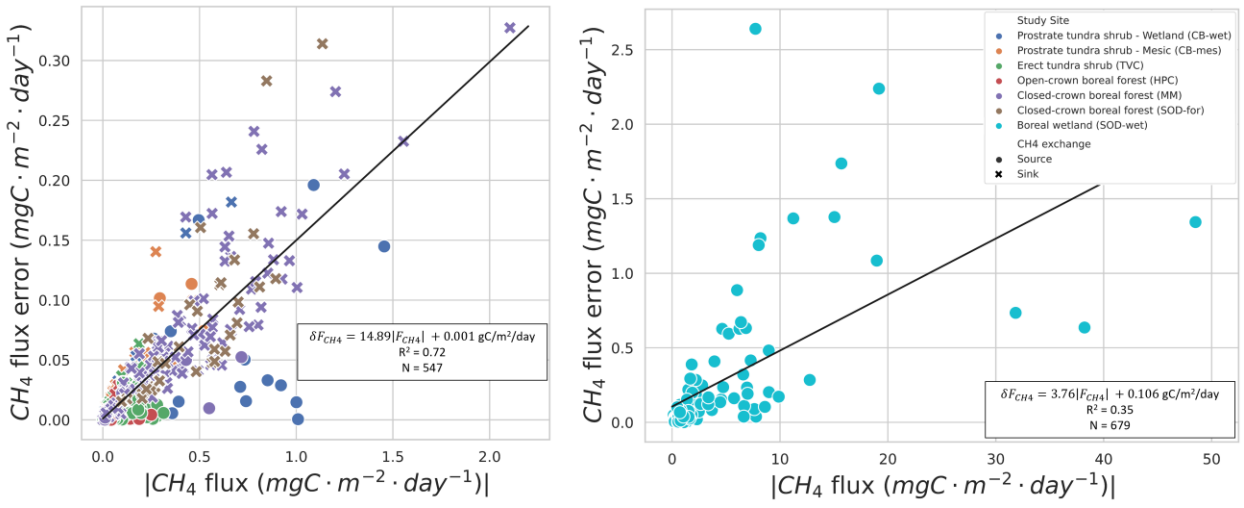

Figure S2. F_{CH4} uncertainty relationship to $|F_{CH4}|$ for the five study sites: Montmorency Forest (MM), Cambridge Bay (CB), Trail Valley Creek (TVC), Havikpak Creek (HPC) and Sodankylä (SOD).

Soil liquid water content calculation

A mix of ice and liquid water can coexist in the soil pore space when soil temperature is around 0 °C. MM and SOD–for are the only sites where the conditions allowed the coexistence of ice and liquid water in the soil pore space of soil upper layers for most of winter. MM was equipped with permanent TEROS 12 Soil Moisture Sensors (METER Group) at 5 cm depth. At SOD–for, instantaneous soil LWC measurements were conducted along with the snow and soil properties using a ML3 ThetaProbe Soil Moisture Sensor (Delta–T Devices). Zhang et al. (2010) empirical soil liquid water and ice mixing model was used to calculate soil volumetric liquid water content (LWC) and ice fraction from permittivity probes:

$$LWC = a \cdot \frac{\rho_b}{\rho_w} \cdot |T_{soil}|^{-b} \quad (5)$$

$$\ln a = 0.5519 \cdot \ln SSA + 0.2618 \;\; ; \;\; \ln b = -0.264 \cdot \ln SSA + 0.3711 \quad (6)$$

where ρ_w and ρ_b (g cm^{-3}) represent liquid water and soil bulk density respectively, T_{soil} (^{o}C) represents soil temperature, SSA (m^{-1}) represents soil particles specific surface area described by Fooladman (2011).

$$SAA = 3.89 \cdot {d_g}^{-0.905} \quad (7)$$

$$\ln d_g = f_c \cdot \ln M_c + f_{si} \cdot \ln M_{si} + f_{sa} \cdot \ln M_{sa} \quad (8)$$

where d_g represents the soil geometric mean particle–size diameter (mm), *f* and M represent soil fractions and mean particle–size diameter (mm) of soil components respectively. The model's soil components are clay (M_c = 0.001 mm), silt (M_{si} = 0.026 mm) and sand (M_{sa} = 1.025 mm).

855 **CH_4 flux across vegetation types at Trail Valley Creek**

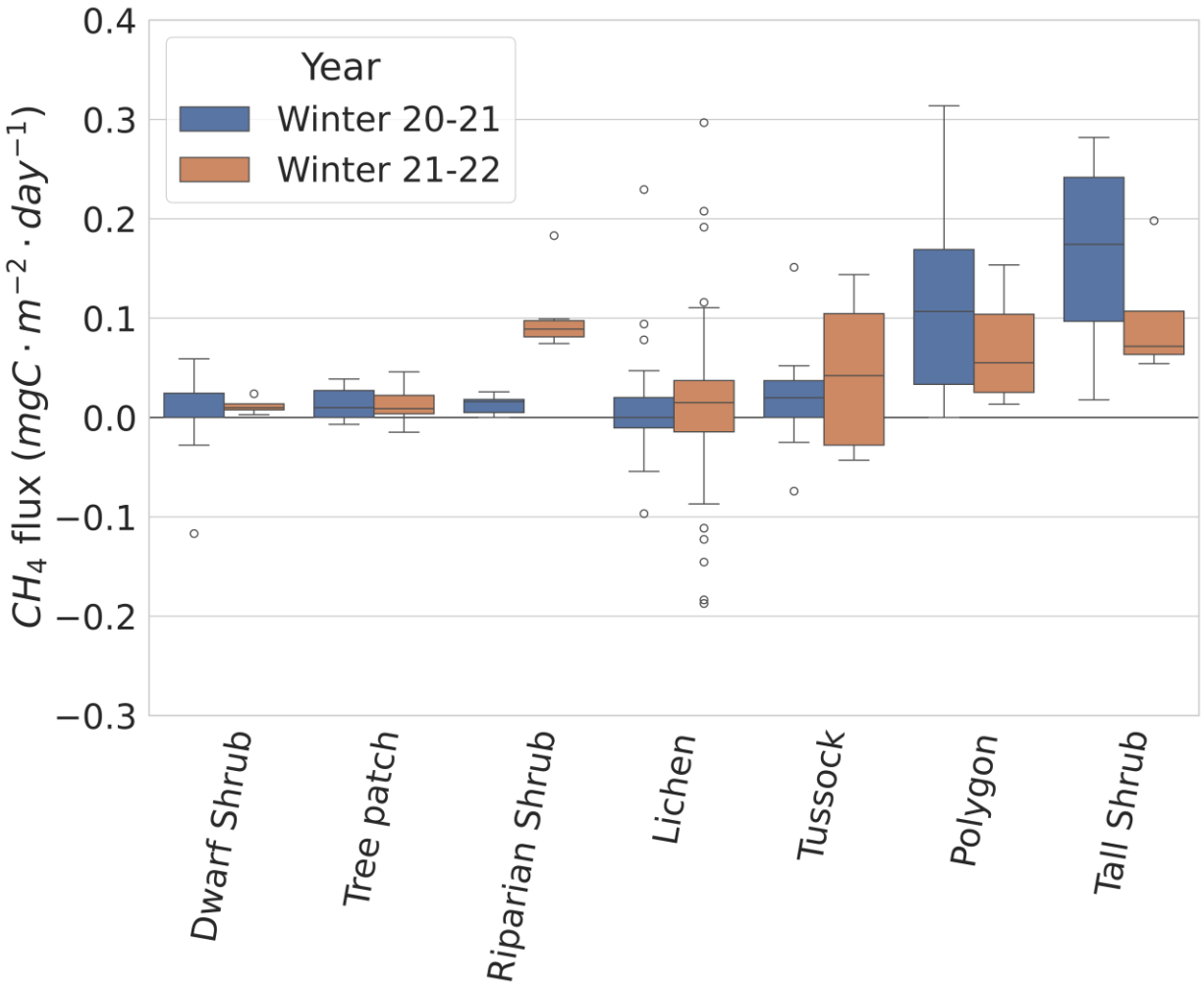

856
857 **Figure S3.** CH_4 flux across vegetation types at Trail Valley Creek. Vegetation types were not
858 distinguished by soil moisture classes (like at the Cambridge Bay study site) since the information
859 was not available at the scale of the sampling locations.

860 **Spatial variability of boreal wetland CH_4 fluxes**

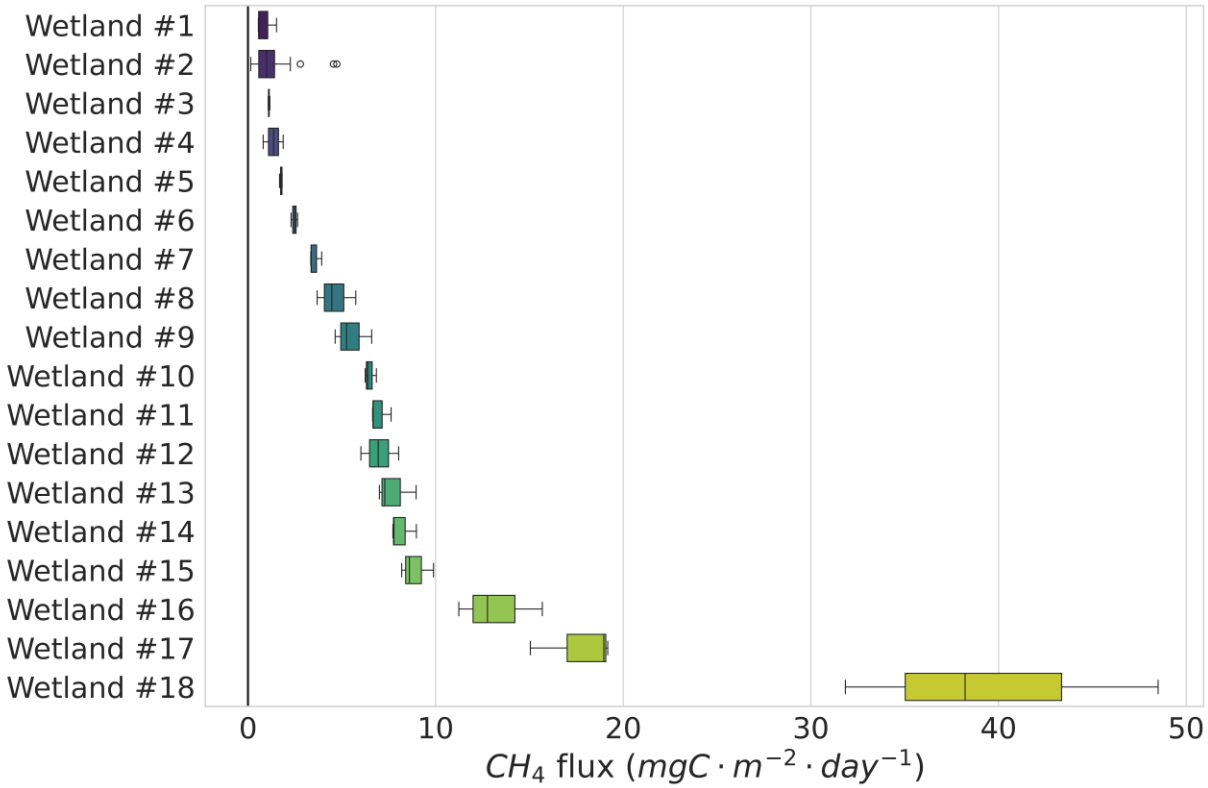

861
862 **Figure S4.** CH_4 flux spatial variability in the boreal wetland at the Sodankylä study site (SOD–
863 wet).

864
865
866
867

CH_4 fluxes relationship to CO_2 fluxes

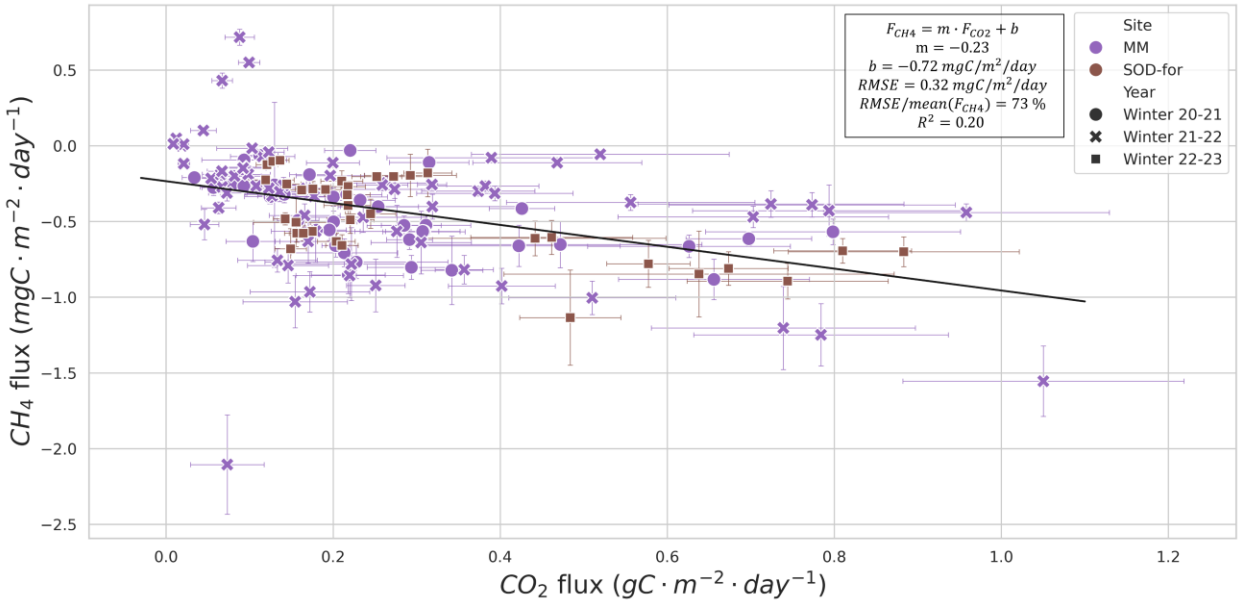

Figure S5. CH_4 flux as a function of CO_2 flux at the Montmorency Forest (MM) and Sodankylä (SOD–for) boreal forest uplands study sites. CO_2 flux data were estimated using the snowpack diffusive gradient method, the same method that was used to obtain the CH_4 flux data in this study. Details about CO_2 flux calculation can be found in Mavrovic et al. (2023).

Boreal forest CO_2 fluxes

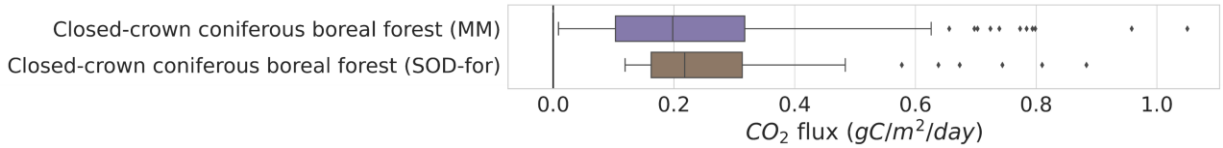

Figure S6. CO_2 flux at Montmorency Forest (MM) during winter 2020–2021 and 2021–2022, and at Sodankylä (SOD–for) during winters 2021–2022 and 2023. CO_2 flux data were estimated using the snowpack diffusive gradient method, the same method that was used to obtain the CH_4 flux data in this study. Details about CO_2 flux calculation can be found in Mavrovic et al. (2023). Outliers were defined as F_{CO2} > Q3 + 1.5 IQR where Q3 is the third quartile and IQR the interquartile range.